PERGAMON

International Journal of Heat and Mass Transfer 42 (1999) 2003–2013

International Journal of
HEAT and MASS
TRANSFER

Experimental evaluation of constants for the Rohsenow pool boiling correlation

I.L. Pioro*

Department of Mechanical Engineering, University of Ottawa, Ottawa, Ontario, Canada K1N 6N5

Received 29 January 1998; in final form 25 August 1998

Abstract

The present experimental study is concerned with heat transfer under nucleate boiling of fluids on the horizontal thick plates made from copper, aluminum, brass and stainless steel. Reported are the results of the effect of the heat flux, the saturation pressure from near atmospheric to vacuum, and the thermophysical properties of four working fluids (water, ethanol, R-113, and R-11) on the heat transfer coefficient under boiling. To quantify the effect of these parameters on the heat transfer coefficient, the Rohsenow pool boiling correlation was used with the constants from the experiment. The experimental data match the data of other investigators. Previous experimental works were analysed to evaluate the prediction intervals of the Rohsenow pool boiling correlation for different surface–fluid combinations. © 1998 Elsevier Science Ltd. All rights reserved.

Key words: Heat transfer; Pool boiling; Two-phase thermosyphon

Nomenclature

c_p	specific heat [J kg K^{-1}]
C_{sf}	coefficient in equations (3) and (5)
D	diameter [m]
D_b	vapour bubble departure diameter [m]
g	acceleration due to gravity [m s^{-2}]
G_b	mass velocity of bubbles at their departure [kg m^{-2} s^{-1}]
f	frequency of vapour bubbles departure [s^{-1}]
h	heat transfer coefficient [W m^{-2} K^{-1}]
h_{fg}	latent heat of vaporization [J kg^{-1}]
$H_{b\text{-}c}$	distance between boiling and condensing surfaces [mm]
H_{WF}	working fluid level [mm]
k	thermal conductivity coefficient [W m^{-1} K^{-1}]
l_*	characteristic dimension, $[\sigma/g(\rho-\rho_g)]^{0.5}$ [m]
L	length [m]
p	pressure [Pa]
R_a	roughness arithmetic average [μm]
R_q	roughness root mean square (rms) [μm]
q	heat flux [W m^{-2}]
T	temperature [°C]
u	velocity [m s^{-1}]
V	volume [m^3].

Greek symbols

δ	wall thickness [m]
Δ	difference
μ	dynamic viscosity [Pa s]
ρ	density [kg m^{-3}]
σ	surface tension coefficient [N m^{-1}].

Subscripts

ave	average
b	boiling
conv	convective
ext	external
f	fluid
g	vapour
h	heated
ID	inside diameter
int	internal
OD	outside diameter
s	surface
sat	saturation

---

* Tel.: (613) 562-5800 ext. 6292; fax: (613) 562-5177; e-mail: ipioro@locutus.cc.uottawa.ca

0017–9310/99/$ - see front matter © 1998 Elsevier Science Ltd. All rights reserved
PII: S0017-9310(98)00294-4

WF working fluid
Physical properties with no subscript refer to saturated liquid.

Dimensionless numbers
Nu_b bubble Nusselt number, $h_b D_b/k$
Pr Prandtl number, $c_p \mu/k$
Re_b bubble Reynolds number, $G_b D_b/\mu$.

Abbreviations
Al aluminum
Cr chromium
Cu copper
DC direct current
E ethanol
G generator
M methanol
Pt platinum
R refrigerant
St. St. stainless steel
W water.

1. Introduction

During the last 70 years, heat transfer under boiling has been investigated by many scientists worldwide. Many theoretical and empirical correlations have been proposed to estimate the heat transfer coefficients as well as critical heat fluxes under boiling in different conditions [1]. The classical case for the boiling process is nucleate boiling on a surface submerged in a liquid pool (conditions of pool boiling). Many varieties of boiling surfaces (plates [2–12], strips [13], wires [9, 14, 15], and single tubes [16]) have been used. In [17], forced convective boiling inside a vertical tube was used to estimate the heat transfer coefficient under pool boiling. The saturation pressure ranged from near atmospheric to critical.

Analysis of these earlier works shows that the main parameters that affect the heat transfer coefficient under pool boiling are heat flux, saturation pressure, thermophysical properties of the working fluid, and some characteristics of the boiling surface material (thermophysical properties, dimensions, thickness, surface finishing, micro-structure, etc.).

Horizontal extended flat surfaces having a square area of at least more than 50–70 cm^2 and a thickness of at least more than 5–6 mm have been seldom investigated (actually, such surfaces have fewer side effects on the heat transfer coefficient associated with a small size surface, thickness, curvature, non-uniformity of void fraction near surface, etc.). Cichelly and Bonilla [2] reported on pool boiling experiments on a relatively large flat circular surface ($D = 102$ mm), but a compound one (0.051 mm of polished chromium was electroplated on a thick copper circular plate). It is known that not only the properties of the boiling surface but also the properties of the underlying material can affect the heat transfer coefficient [1]. That is why such surface made analysis of the boiling process more complicated.

Analysis of the papers devoted to the pool boiling process shows that their main focus is on the effects of thermophysical properties, shape, thickness, orientation in space, and finishing of the boiling surface. Some researchers [9, 18, 19] considered that for many practical cases the effects of these parameters on the heat transfer coefficient are insignificant, except for the boiling of cryogenic fluids, and can be neglected. Others [2–6, 8, 10, 11, 17, 20–27] considered that these effects are significant and proposed different methods to estimate them.

The standard method [20] includes applying a proper constant in the pool boiling correlation according to the surface–fluid combination. Some works [12, 21] showed that the values of exponents in dimensionless numbers in the pool boiling correlation can be varied according to the surface finishing, pressure range, etc. About 40–50 surface–fluid combinations have been investigated and constants for the Rohsenow pool boiling correlation have been evaluated. At first, Rohsenow [20] proposed using the constant values of the exponents in dimensionless numbers for all surface–fluid combinations. However, later he recommended using a value of the exponent in the Prandtl number equal to 1 for water and equal to 1.7 for other fluids. Vachon et al. [21] found that this value varies for different fluids from 0.8–2, and that the value of the exponent in a dimensionless number containing the heat flux also is not constant. In spite of the large number of surface–fluid combinations already investigated, some widely used working fluids (such as ethanol, refrigerants, etc.) and materials of the boiling surface (such as aluminum) were seldom considered. Most handbooks [27–30], reference books [31, 32] and textbooks [33–38] usually present only the surface–fluid combination and corresponding values of the constants, and not the prediction intervals and shape of the surface. This can lead to incorrect application of the Rohsenow pool boiling correlation for heat transfer calculations.

The objectives of the present study are as follows:

(1) Experimental evaluation of the heat transfer coefficients under pool boiling conditions for four widely used working fluids ranging from atmospheric pressure to vacuum, and for four technical surfaces with a wide range of thermal conductivities.
(2) Evaluation of the prediction intervals of the Rohsenow pool boiling correlation for the already known surface–fluid combinations, based on the analysis of previous works.

2. Experiment

The experimental setup consisted of a horizontally flat two-phase thermosyphon, a power supply, a cooling system, a vacuum pump and related instrumentation [1, 10–12]. Two test sections with four boiling surfaces were used during the experiments (Fig. 1). The boiling surfaces (411×51 mm) were made from thick extended plates to avoid the additional effects of the wall thickness and dimensions of the boiling surface on the heat transfer coefficient. The materials for the plates (copper, aluminum, brass and stainless steel) were chosen with different values of thermal conductivity (400–14 W m^{-1} K^{-1}) and with approximately same surface roughness ($R_a = 2 \pm 1.5$ μm or $R_q = 2.5 \pm 2$ μm). Such surface roughness (R_a) can be produced by any of the following common industrial methods: cold rolling; drawing; extruding; die, perm mold, and investment castings; milling; etc. The surface roughness was measured by laser profilometer at Chalk River Laboratories (Canada). The boiling surface of the first test section was machined in the shape of a rectangular cavity inside an aluminum plate, and then the plate was oxidized. The boiling surfaces of the second test section were made of brass plate, which later was replaced by stainless steel SS304 plate and then copper plate. All plates were exposed to the surrounding air before being installed inside the thermosyphon, and so the copper plate was naturally oxidized. The brass and stainless steel plates did not show any visible signs of oxidation. The upper parts of the test sections were cooling jackets. The heater for the test sections was made from a stainless steel SS304 strip, 0.45 mm thick, 411 mm long and 51 mm wide, which was heated by direct electrical resistance. The heater was electrically insulated with thin (1.8 mm) Pyrex glass from the heating plates and thermally insulated from surrounding air. The heater's multilayer thermal insulation consisted of thick Pyrex glass (4.8 mm), refractive aluminum foil, two sheets of mineral wool (6.4 mm each), and solid plastic (13.7 mm). Solid plastic was pressed towards the heating plate by means of 26 plastic bolts for proper contact between heater, thin Pyrex glass and heating plate. The heater was provided with an electrical power supply rated up to 120 V at 3000 A DC. The heating part of a test section was installed inside a ply-wood box with 25 mm walls and the test section was covered with fiberglass insulation (except for the sides of the Teflon and the transparent Acrylic inserts) to prevent heat loss. For some heat flux ranges two guard flexible silicon rubber fiberglass insulated heaters (Model No. SRFG-208/10 OMEGA, 50.8×203.2 mm ($2 \times 8''$), $q = 15.5$ kW m^{-2} (10 W in.$^{-2}$)) installed between two mineral wool sheets were employed. A total of nine sheathed chromel–alumel thermocouples (Model No. KMTSS-125G-6 OMEGA, subminiature transition joint probes, type-K, 3.2 mm (0.125″) outside diameter stainless steel sheath, 152 mm (6″) length, grounded junc-

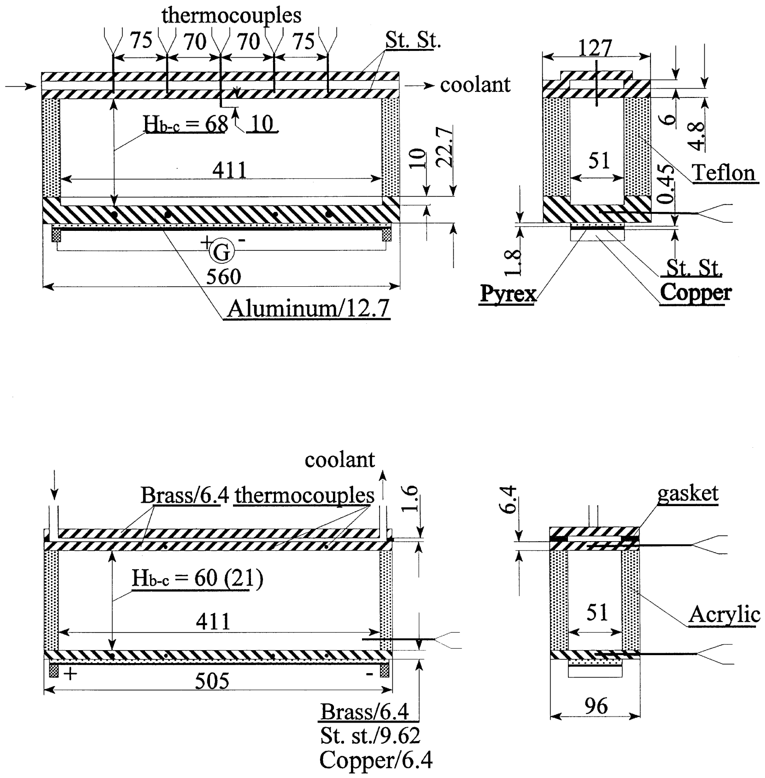

Fig. 1. Test sections.

tion) were used, as shown in Fig. 1. All thermocouples were calibrated in situ. The thermocouples were installed inside the metal plates from their long sides: four into the heating plate (boiling surface) and four into the cooling plate (condensing surface), with the distances between the thermocouples being about 70–75 mm. The measuring ends of the thermocouples were on the central vertical plane. All thermocouples were installed through Swagelok tube fittings screwed into metal plates for proper contact between measuring ends and plate internal surface. The thermocouple used to measure the saturation temperature was installed inside the thermosyphon. Coolant (antifreeze mixture) at a given temperature was provided through a Colora-supercryostat cooling system. For a given series of experiments, a given amount of the working fluid was charged at a vacuum of about 10^{-3} torr (0.133 Pa). Working fluids were degassed before charging into the chamber. Four widely used liquids with quite different thermophysical properties (water, ethanol, R-113 and R-11) were chosen as the working fluids. All tests reported here were done at steady state and on clean boiling surfaces (the experimental surface was cleaned with acetone and then washed with the working fluid).

The heat loss was about 3–5% of the total input and the uncertainties in instrument readings, thermocouples locations, and calculating a thermal conductivity coefficient of the heating plate were not more than 3%. The total inaccuracy of the experiments did not exceed 8%, that is usual for such type of experiments [2, 4, 26].

3. Analysis

Analysis of the experimental data requires the appropriate selection of variables which, for the present case, would affect the heat transfer coefficient. For this particular work it was decided to apply the method of correlating heat transfer data for the surface boiling of liquids proposed by Rohsenow in 1952 [20]. The main concept of this method is that the heat transfers from the wall directly to the liquid with an increased heat transfer rate, due to the agitation of liquid by the departing vapour bubbles. Based on this logical explanation of the boiling heat transfer mechanism, the usual type of convective heat transfer equation was used

$$Nu_\mathrm{b} = C_1 \cdot Re_\mathrm{b} \cdot Pr, \tag{1}$$

where C_1 is the constant and all thermophysical properties of the fluid are evaluated at the saturation temperature corresponding to the saturation pressure in the system.

Equation (1) can be written using the following expression:

$$\frac{Re_\mathrm{b} \cdot Pr}{Nu_\mathrm{b}} = \frac{c_\mathrm{p} \cdot \Delta T_\mathrm{b}}{h_\mathrm{fg}}, \tag{2}$$

in the final form:

$$\frac{c_\mathrm{p} \cdot \Delta T_\mathrm{b}}{h_\mathrm{fg}} = C_\mathrm{sf}\left[\frac{q}{\mu \cdot h_\mathrm{fg}}\sqrt{\frac{\sigma}{g \cdot (\rho - \rho_\mathrm{g})}}\right]^m \left(\frac{c_\mathrm{p} \cdot \mu}{k}\right)^n, \tag{3}$$

where C_sf is constant, depending upon the nature of the heating surface–fluid combination.

4. Results and discussion

The results show the effect of the heat flux, the saturation pressure, the thermophysical properties of four working fluids (water, ethanol, R-113 and R-11) and the four technical surfaces (copper, aluminum, brass and stainless steel) on the average heat transfer coefficient. In this research the average boiling heat transfer coefficient is defined as

$$h_\mathrm{b} = \frac{q}{T_\mathrm{b\,ave} - T_\mathrm{sat}}, \tag{4}$$

where $T_\mathrm{b\,ave}$ is the average wall temperature on the boiling surface calculated according to the measured temperatures inside the heating plate.

The first step in this work was to find the effect of the height of the working fluid level on the heat transfer coefficient under boiling conditions. This effect was mainly described in [1, 10, 11]. Based on analysis of the experimental data, and on visual studies, two conclusions can be made:

1. for the working regime (that is developed nucleate boiling with a uniform temperature distribution over the entire boiling surface), at least 50 ml ($H_\mathrm{WF} = 2.4$ mm) of working fluid must be charged; and
2. in a wide range of filling charges ($H_\mathrm{WF} \geqslant 2.4$ mm), the heat transfer coefficient is almost independent of this parameter, or changed negligibly.

That is why the majority of the experiments with the aluminum heating plate were carried out in a working fluid of 50 ml ($H_\mathrm{WF} = 2.4$ mm), and with other boiling surfaces (brass, stainless steel, and copper) $V_\mathrm{WF} = 120$ ml ($H_\mathrm{WF} = 5.8$ mm).

According to the form of equation proposed by Rohsenow [20], the first main series of experiments were performed under the constant values of saturation temperature, to determine the primary effect of the heat flux on the heat transfer coefficient. For all surface–fluid combinations and in a wide range of saturation temperature, exponent $m \approx 0.33$. This conclusion matches the majority of experimental data by other researchers.

The second main series of experiments investigated the effects of the saturation temperature and the working

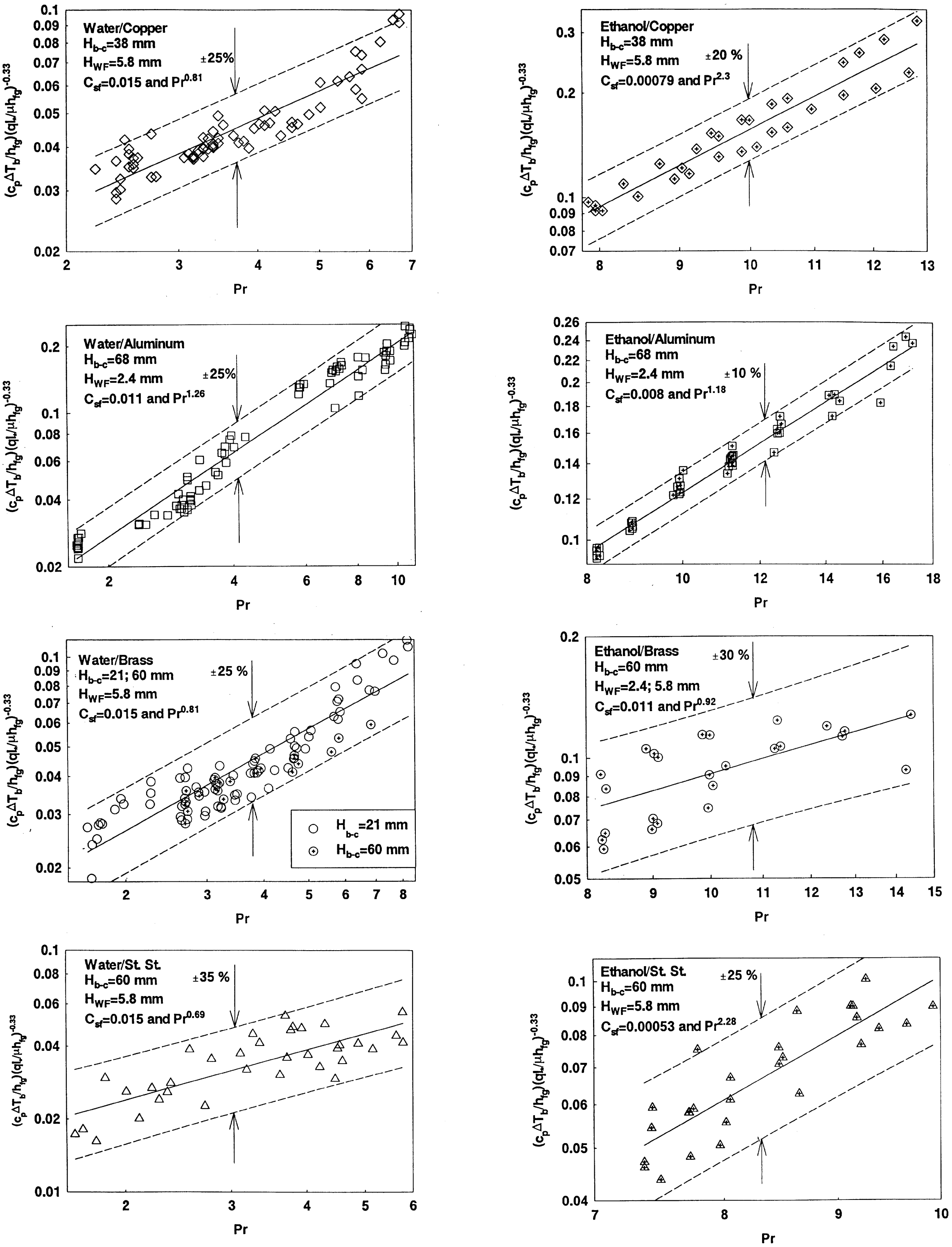

Fig. 2. Correlation of experimental data.

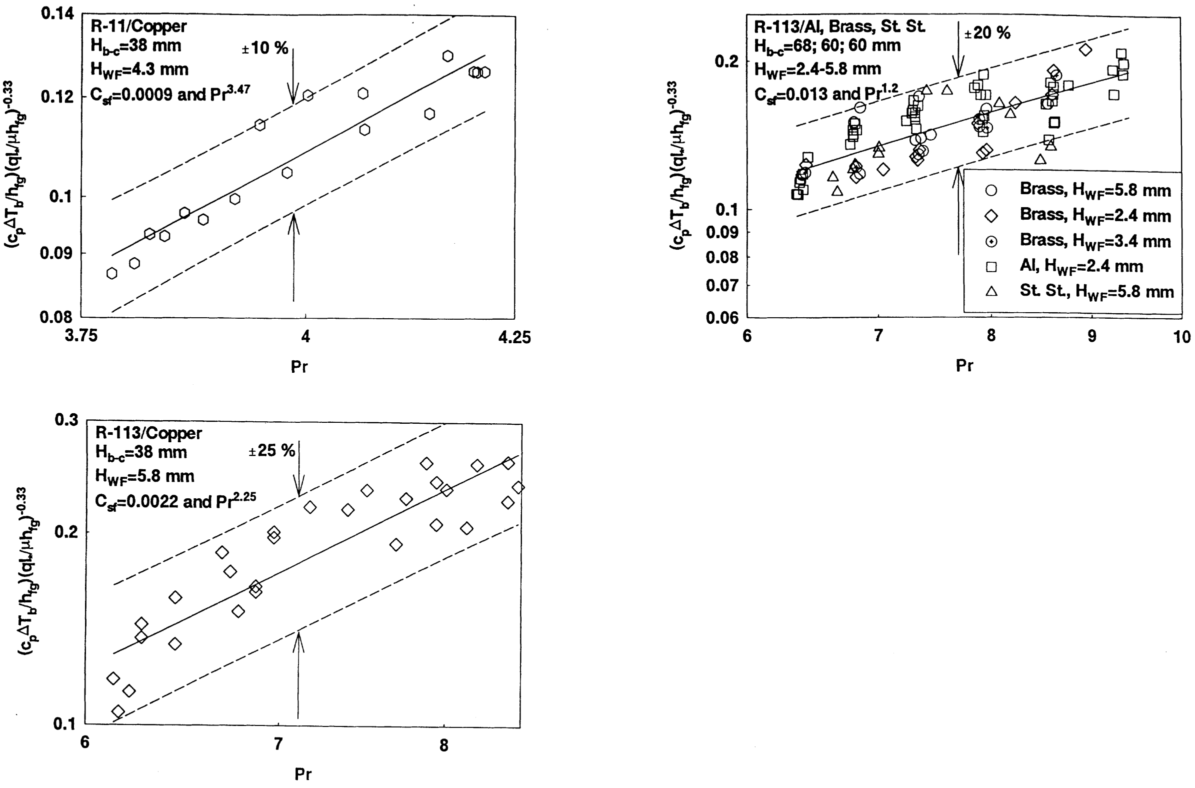

Fig. 2. (*Continued*)

fluid's thermophysical properties (mainly the effect of the Prandtl number) on the heat transfer coefficient. The primary experimental data are shown in [10, 11]. The recalculated data in the non-dimensional form are shown in Figs 2 and 3 (Fig. 2; present data, Fig. 3; data of Cichelly and Bonilla [2], because theirs are the only data obtained under similar conditions and in a similar test section design).

Based on the above discussion, the final form of the generalized correlation is:

$$\frac{c_\mathrm{p}\cdot\Delta T_\mathrm{b}}{h_\mathrm{fg}} = C_\mathrm{sf}\left[\frac{q}{\mu\cdot h_\mathrm{fg}}\sqrt{\frac{\sigma}{g\cdot(\rho-\rho_\mathrm{g})}}\right]^{0.33}\left(\frac{c_\mathrm{p}\cdot\mu}{k}\right)^{n}, \tag{5}$$

where the values of C_sf and exponent n are listed in Table 1 for all investigated surface–fluid combinations, together with some other cases where primary experimental data were available.

Figure 4 shows some of the water–surface combinations from Table 1 in the same co-ordinates. From Fig. 4 it is clear that the present experimental data (lines W/Al, W/Cu, W/Brass, and W/St. St.) match the data for the boiling of water on a chromium flat surface [2], and match the data for the boiling of water on platinum wire [14] under atmospheric pressure. With the pressure decreasing from atmospheric, boiling started to be irregular, with fewer vapour bubble generating centers, especially on the boiling surfaces that had high thermal conductivity. This leads to a decreasing heat transfer coefficient under pool boiling conditions.

A possible explanation for this effect is as follows. During the formation and growth of a vapour bubble, the work of bubble creation must be complete. If overheating of the surface and some other conditions are not enough to create a vapour bubble that has a radius greater than critical, the vapour bubble can not exist. With decreasing saturation pressure, the diameters of the vapour bubbles increase significantly, as well as the work for their creation. For surfaces that have high values of thermal conductivity, the overheating around a nucleation site will spread easily over the entire surface, and the minimum conditions for vapour bubble formation and growth will not be achieved. As a result, the boiling surface will be depleted with active nucleation sites, and heat will be transferred from the surface mainly by natural convection under a higher average temperature difference, and therefore under lower values of heat transfer coefficient. Boiling will become more unstable and irregular. This explanation is fully supported by visual observations of the boiling process. For surfaces with low values of thermal conductivity, it is easier to reach local overheating and to create a vapour

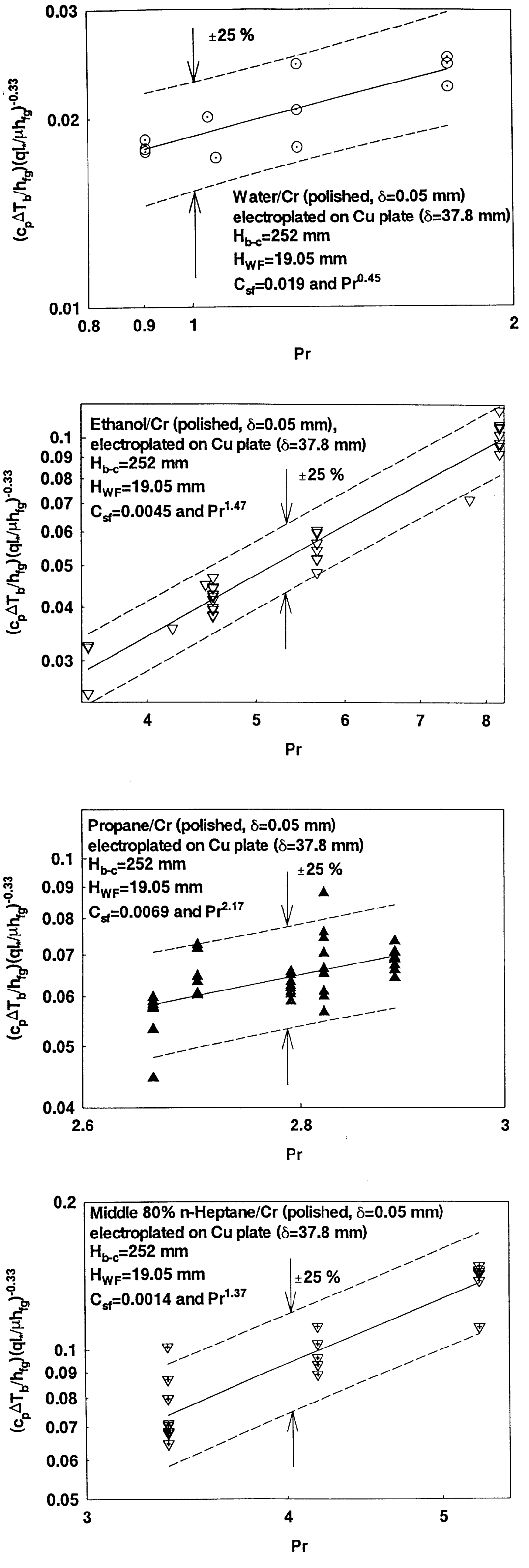

Fig. 3. Correlation of experimental data obtained in [2].

bubble. It is known that water is the fluid that has the largest sizes of vapour bubbles for the constant value of saturation pressure, and that is why with decreasing saturation pressure the effect of thermal interaction between growing bubbles and the boiling surface material increased significantly (Fig. 4, lines: W/Al, W/Brass and W/St. St.). For values of saturation pressure close to the atmospheric ($Pr \approx 1.75$), this effect becomes insignificant, due to the relatively small sizes of vapour bubbles, high frequency of vapour bubble generation and high density of active vapour bubble generating centers (Table 2). This phenomenon, which is connected with the appearance of the heat fluxes inside the wall and acting along the boiling surface, is called the conjugate effect. Such conjugate heat transfer problems can be found in many single- and two-phase flow conditions [1, 42].

The experimental data for water boiling on a horizontal brass tube (Fig. 4, line W/Brass$_{\text{tube}}$ [16]) differ from the data for water boiling on a brass plate. A possible explanation for this could be the additional agitation of the boundary layer of the above surfaces by the departed vapour bubbles from the lower parts of the tube.

Also, together with the conjugate, shape and orientation in space effects, the effect of the surface finishing and microstructure must be accounted for. For this reason, the oxidized copper surface (Fig. 4, line W/Cu) shows higher values of heat transfer coefficient than were expected.

Figure 5 shows some other fluid–surface combinations. The same explanation as for water can be applied to ethanol, because ethanol has internal boiling characteristics that are close to those of water (Table 2). Unlike water and ethanol, the behaviour of R-113 (the smallest sizes of vapour bubbles, lower values of heat of evaporation, high vapour generating frequency and high density of active centers) under boiling on different surfaces (except for copper) shows that the conjugate effect is negligible for the entire experimental range.

5. Conclusions

(1) The values of constants in the Rohsenow pool boiling correlation were experimentally evaluated for 13 surface-fluid combinations.
(2) The work of other researchers was analysed to evaluate the prediction intervals for the Rohsenow pool boiling correlation for other surface–fluid combinations.
(3) The effect of the working fluid level on the heat transfer coefficient is significant for flat horizontal boiling surfaces in the range less than 2.4 mm.
(4) The effect of the thermophysical properties of a boiling surface (conjugate effect) on the heat transfer coefficient under pool boiling increases with decreasing saturation pressure, from atmospheric pressure.

Table 1
Average values of constants in the Rohsenow pool boiling correlation and prediction intervals

Fluid/Surface 1	C_{sf} 2	n 3	T_{sat}, °C 4	ΔT_b, °C 5	q, kW m^{-2} 6	h_b, kW $m^{-2}K^{-1}$ 7
Water/Copper (plate oxidized, $R_a = 1.37$, $R_q = 1.73$)	0.015	0.81	23–82	4.2–14	1.8–72.3	0.26–6.1
Water/Copper (thin circular plate emery polished and paraffin treated) [5]	0.0147[21]	1	100	9.4–18.3	41–950	3.7–57
Water (int forced conv)/Copper (vertical tube) [17]	0.013	1.7	100	4–15	18–190	4.5–12.7
Water/Copper (circular plate emery polished) [4]	0.0128[21]	1	100	5.5–15.5	28–530	3.4–34
Water/Copper (circular plate scored) [8]	0.0068[21]	1	100	1.7–8.3	1.6–190	8.5–19
Water/Aluminum (circulate plate polished, $R_q = 0.33$) [6]	0.011[Pioro]	1	100	5–8.3	28–126	5.6–15.1
Water/Aluminum (plate oxidized, $R_a = 3.61$, $R_q = 4.52$)	0.011	1.26	3.5–103	5–22	1.3–90	0.1–10
Water/Brass (plate, $R_a = 0.47$, $R_q = 0.66$)	0.015	0.81	14–103	4–15	1.2–144	0.2–11
Water/Brass (tube ext) [16]	0.009[Pioro] 0.006[20]	1.1 1.7	28–112	2.3–14	8–43	1–11
Water/Chromium (polished thin layer on circular copper plate) [2]	0.019[Pioro]	0.45	100–205	8–18	140–655	14.6–51
Water/Platinum (wire) [14]	0.013[27]	1	100–355	1–28	3–3200	1.8–480
Water/St. St. (plate, $R_a = 0.75$, $R_q = 1.2$)	0.015	0.69	30–103	4–13	5–40	1–6.2
Water/St. St. (circular plate polished, $R_q = 0.13$) [6]	0.01[Pioro]	1	100	4.4–7.2	28–126	6.4–17.5
Water/St. St. (circular plate grounded, $R_q = 0.53$) [6]	0.008[Pioro]	1	100	3.3–6.7	22–158	6.7–23.6
Water/St. St. (circular plate grounded, $R_q = 3.6$) [6]	0.007[Pioro]	1	100	3.3–5.6	37–160	11.5–29
Water/St. St. (thin strip pitted with Teflon coating in pitts) [13]	0.0058[21]	1	100	0.5–8.3	1.6–265	3.1–31.8
Ethanol/Copper (plate oxidized, $R_a = 1.37$, $R_q = 1.73$)	0.00079	2.3	30–82	13–20.2	2.1–26	0.1–2
Ethanol/Aluminum (plate oxidized, $R_a = 3.61$, $R_q = 4.52$)	0.008	1.18	16–78	11–21	2.7–32	0.16–2.3
Ethanol/Brass (plate, $R_a = 0.47$, $R_q = 0.66$)	0.011	0.92	40–78	9–14	4.3–56	0.7–4.7
Ethanol/Chromium (polished thin layer on circular copper plate) [2]	0.0045[Pioro] 0.0027[20]	1.47 1.7	78–210	3–34	15–800	3.2–72
Ethanol/St. St. (plate, $R_a = 0.75$, $R_q = 1.2$)	0.00053	2.28	49–90	7–14	10–45	0.7–6
Methanol/Brass (tube ext) [16]	0.0026	1.7	13–72	5–19	7.8–43	0.7–6
iso-Propanol (int forced conv)/Copper (vertical tube) [17]	0.0022	1.7	82.5	5–20	5.7–95	1.1–4.75
n-Butanol (int forced conv)/Copper (vertical tube) [17]	0.003	1.7	117	7–17	9.5–95	1.4–5.6
R-11/Copper (plate oxidized, $R_a = 1.37$, $R_q = 1.73$)	0.0009	3.47	23–49	6.4–11.2	1.4–12	0.22–1.2
R-12/Copper (tube ext) [39]	0.016[Pioro]	1.7	2–15	6.6–10	1.5–5	0.2–0.5
R-113/Copper (plate oxidized, $R_a = 1.37$, $R_q = 1.73$)	0.0022	2.25	32–80	9–16	3.2–21	0.24–1.9
R-113/Aluminum (plate oxidized, $R_a = 3.61$, $R_q = 4.52$), Brass (plate, $R_a = 0.47$, $R_q = 0.66$), St. St. (plate, $R_a = 0.75$, $R_q = 1.2$)	0.013	1.20	20–71	6–15	1.3–24	0.2–2
CCl_4 (int forced conv)/Copper (vertical tube) [17]	0.013	1.7	76.7	10–28	5.5–63	0.55–2.3
CCl_4/Copper (circular plate emery polished) [4]	0.007[21]	1.7	76.7	12–22	10.2–194	0.85–14
CCl_4/Copper (circular plate lapped) [7]	0.0031[21]	1.7	76.7	8–13	22–280	2.6–25
CCl_4/Brass (tube ext) [16]	0.0022[Pioro]	2.1	33–86	6.5–25	7.8–43	0.6–4
Propane/Chromium (polished thin layer on circular copper plate) [2]	0.0069[Pioro]	2.17	34–83	3.3–22	27–400	8–28
n-Pentane/Copper (circular plate mirror finishing) [7]	0.0171[21]	1.7	36	16.7–44.4	22–252	1.3–5.7

Table 1
(*Continued*)

Fluid/Surface 1	C_{sf} 2	n 3	T_{sat}, °C 4	ΔT_b, °C 5	q, kW m^{-2} 6	h_b, kW m^{-2}K^{-1} 7
n-Pentane/Copper (plate emery polished, $R_q = 0.15$) [26]	0.0154[21]	1.7	36	17–22	15–90	0.85–4
n-Pentane/Copper (circular plate emery rubbed) [7]	0.0074[21]	1.7	36	6.7–15.6	31.5–284	4.7–18.2
n-Pentane/Copper (circular plate lapped) [7]	0.0049[21]	1.7	36	5–8.3	31.5–284	6.3–34
n-Pentane/Zinc (circular plate polished) [3]	0.0088[21]	1.7	36	4–38	6.3–284	1.6–7.5
n-Pentane/Chromium (polished thin layer on circular copper plate) [2]	0.015[20]	1.7	48–147	4–31	29–440	2–35
n-Pentane/Nickel (circular plate mirror finishing) [7]	0.0154[21]	1.7	36	6.1–9.4	28–284	4.6–30.2
n-Pentane/Nickel (plate emery polished) [26]	0.0127[21]	1.7	36	11–22	13–112	0.85–5.7
n-Pentane/Nickel (circular plate lapped) [7]	0.0043[21]	1.7	36	15.5–39	31.5–284	2–7.3
n-Pentane/Inconel (circular plate mirror finishing) [7]	0.018[21]	1.7	36	19.4–43.3	31.5–221	1.6–5.1
n-Pentane/Inconel (circular plate lapped) [7]	0.0072[21]	1.7	36	9.4–15.6	31.5–252	3.4–16.2
Benzene/Chromium (polished thin layer on circular copper plate) [2]	0.01[20]	1.7	80–214	4–45	25–600	2.5–41
n-Heptane/Chromium (polished thin layer on circular copper plate) [2]	0.0014[Pioro]	1.37	95–185	10–32	40–440	2.8–25
Acetone/Copper (circular plate emery polished) [4]	0.0096[Pioro]	1.7	56	14.4–22.2	16.4–252	1.1–11.4
35% K_2CO_3 (int forced conv)/Copper (vertical tube) [17]	0.0054	1.7	106	8–15	19–95	2.4–6.3
50% K_2CO_3 (int forced conv)/Copper (vertical tube) [17]	0.0028	1.7	72.4	10–17	25–95	2.5–5.6

Fluids are listed in the following order: water, alcohols, fluorocarbons (refrigerants), hydrocarbons, and others.

Materials of the surfaces are located according to the value of thermal conductivity: from highest to lowest.

Surfaces of the same material generally are located according to their decreasing value of C_{sf}.

All surfaces are located horizontally except where noted.

Generally, two-phase thermosyphon type chambers were used, with the boiling surface (plates or strips) located at the bottom or immersed in a pool (wires or tubes), and the condensing part located at the top.

In the present work plates (boiling surface 411 × 51 mm) from copper (no surface treatment, naturally oxidized, $\delta = 6.4$ mm, $R_a = 1.37$ μm, $R_q = 1.73$ μm), aluminum (surface machined (milling process) and oxidised, $\delta = 12.7$ mm, $R_a = 3.61$ μm, $R_q = 4.52$ μm), brass (no surface treatment, $\delta = 6.4$ mm, $R_a = 0.47$ μm, $R_q = 0.66$ μm), and SS304 stainless steel (no surface treatment, $\delta = 9.62$ mm, $R_a = 0.75$ μm, $R_q = 1.2$ μm) were used.

In [5], thin circular copper plate ($D = 25.4$ mm, $\delta = 0.5$ mm) was used.

In [17], vertical copper tube ($D_{ID} = 27.1$ mm, $\delta = 6.2$ mm, $L_h = 1.18$ m) was used with forced convective boiling of working fluid (u = 0.24–1.1 m/s). The pool boiling heat transfer coefficient was obtained by subtraction of convective part from the measured value of heat transfer coefficient.

In [4], copper circular plate ($D = 76.2$ mm) was used.

In [8], copper circular plate ($D = 50.8$ mm, $\delta = 6.4$ mm) was used.

In [6], circular aluminum and stainless steel plates ($D = 76.2$ mm) were used.

In [16], brass horizontal tube sealed from both ends ($D_{OD} = 38.1$ mm, $\delta = 6.35$ mm, $L_h = 115.9$ mm) was immersed in a pool.

In [2], thick copper circular plate ($D = 101.6$ mm, $\delta = 37.8$ mm) with 0.051 mm of polished electroplated chromium was used. $H_{WF} = 19.05$ mm.

In [14], platinum wires ($D = 0.3$; 0.6; and 1.2 mm) immersed in a pool were used.

In [13], thin stainless steel SS304 strips (140 × 30.5 mm, $\delta = 0.25$ mm) were used.

In [39], copper tube ($D_{OD} = 19.05$ mm, $\delta = 1.65$ mm, $L_h = 91.4$ mm) was used.

In [7], circular plates ($D = 50.8$ mm) from copper, nickel, and Inconel were used.

In [26], films of copper and nickel plated on a rectangular copper heater (101.6 × 19.05 mm) were used.

In [3], circular plate ($D = 19.1$ mm) was used. $H_{WF} = 5.6$ mm.

The typical range of surface roughness [40] produced by polishing process is about $R_a = 0.1$–0.4 μm; by lapping—$R_a = 0.05$–0.4 μm; by superfinishing—$R_a = 0.025$–0.2 μm. The representative value of surface roughness (R_a) for a drawn tubing is about 1.5 μm [41].

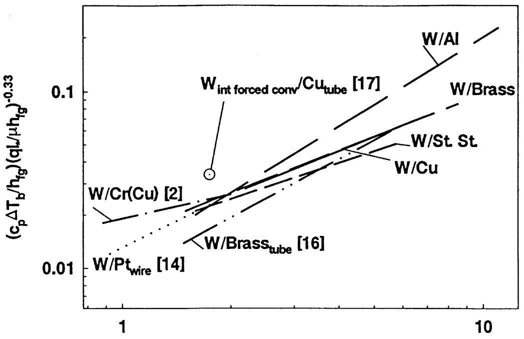

Fig. 4. Comparison of data for different water–surface combinations: surface material without subscript refers to rectangular or circular plates [2] (for details see Table 1).

Table 2
Average values of boiling internal characteristics [1]

Fluid	Water			Ethanol			R–113		
p_{sat}, bar	1	0.5	0.2	1	0.5	0.2	1	0.5	0.2
T_{sat}, °C	100	83	60	78	65	46	48	28	8
D_b, mm	2.3	5.4	13.3	1.1	2.4	7	0.4	1.1	2.2
f, s^{-1}	67	43	22	112	100	67	100	100	100

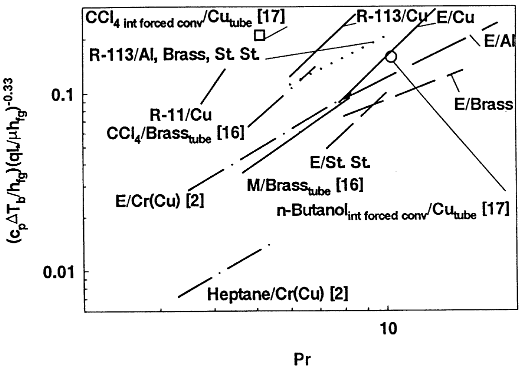

Fig. 5. Comparison of data for different fluid–surface combinations: surface material without subscript refers to rectangular or circular plates [2] (for details see Table 1).

(5) Based on our experimental data, as well as on other investigations, the conjugate effect can be found under boiling in different conditions, and as a result the conjugate effect must be accounted for in boiling.

Acknowledgement

The author would like to express his appreciation to Dr. S. Doerffer (Chalk River Laboratories, Canada) for his valuable comments on this article.

References

[1] L.S. Pioro, I.L. Pioro, Industrial Two-Phase Thermosyphons, Chapter 2, Begell House, New York, 1997.

[2] M. Cichelly, C. Bonilla, Heat transfer to liquids boiling under pressure, Transactions of AIChE 41 (1945) 755–787.

[3] H.B. Clark, P.S. Strenge, J.W. Westwater, Active sites of nucleate boiling, Chemical Engineering Progress Symposium Series (1959) 55 (29) 103–110.

[4] H.M. Kurihara, J.E. Myers, The effects of superheat and surface roughness on boiling coefficients, Journal of AIChE (1960) 6 (1) 83–86.

[5] P. Griffith, J.D. Wallis, The role of surface conditions in nucleate boiling, Chemical Engineering Progress Symposium Series, (1960) 56 (30) 49–63.

[6] S.T. Hsu, F.W. Schmidt, Measured variations in local surface temperatures in pool boiling of water, Journal of Heat Transfer (1961) 83 254–260.

[7] P.J. Berenson, Experiments on pool-boiling heat transfer, International Journal of Heat and Mass Transfer (1962) 5 985–999.

[8] C.F. Bonilla, J.J. Grady, G.W. Avery, Pool boiling heat transfer from scored surfaces, Chemical Engineering Progress Symposium Series (1965) 61 (57) 280–288.

[9] V.I. Tolubinskiy, Heat Transfer under Boiling, Chapter 5, (In Russian), Naukova Dumka, Kiev, 1980.

[10] Y. Lee, I. Pioro, H.J. Park, An experimental study on a plate type two-phase closed thermosyphon, in: Proceedings of the 4th International Heat Pipe Symposium, Tsukuba, Japan, May, 1994, pp. 49–58.

[11] I.L. Pioro, H.J. Park, Y. Lee, Heat transfer in a two-phase closed thermosyphon: horizontally flat plate type, in: Proceedings of the 5th International Symposium on Thermal Engineering and Science for Cold Regions, Ottawa, Canada, May, 1996, pp. 489–494.

[12] I. Pioro, Boiling heat transfer characteristics of thin liquid layers in a horizontally flat two-phase thermosyphon, Preprints of the 10th International Heat Pipe Conference, Stuttgart, Germany, September, Paper H1-5 (1997).

[13] R.K. Young, R.L. Hammel, Higher coefficients for heat transfer with nucleate boiling, Chemical Engineering Progress Symposium Series (1965) 61 (59) 264–270.

[14] J.N. Addoms, Heat transfer at high rates to water boiling outside cylinders, D.Sc. Thesis, Chemical Engineering Department, Massachusetts Institute of Technology, MA, June, 1948.

[15] E.A. Farber, E.L. Scorah, Heat transfer to water boiling under pressure, Transactions of ASME (1948) 70 369–384.

[16] D.S. Cryder, A.C. Finalborgo, Heat transmission from metal surfaces to boiling liquids: effect of temperature of liquid on liquid film coefficient, Transactions of AIChE 1937 (50) 346–362.

[17] E.L. Piret, H.S. Isbin, Natural-circulation evaporation two-phase heat transfer, Chemical Engineering Progress (1954) 50 (6) 305–311.

[18] S.S. Kutateladze, V.M. Borishanskii, A Concise Encyclopedia of Heat Transfer, Chapter 12, Pergamon Press, New York, 1966.

[19] D.A. Labuntsov, Heat transfer problems with nucleate boiling of liquids, Thermal Engineering (1972) 9 21–28.

[20] W.M. Rohsenow, A method of correlating heat transfer data for surface boiling of liquids, Transactions of ASME (1952) 74 969–976.

[21] R.I. Vachon, G.H. Nix, G.E. Tanger, Evaluation of constants for Rohsenow pool-boiling correlation, Journal of Heat Transfer (1968) 90 239–247.

[22] A.A. Watwe, A. Bar-Cohen, The role of thickness and thermal effusivity in pool boiling critical heat flux in highly-wetting liquids, in: Proceedings of the 10th International Heat Transfer Conference, Vol. 5, Brighton, England, 1994, pp. 183–188.

[23] P. Sadasivan, C. Unal, R. Nelson, Pool boiling on thin heaters: the role of thermal interaction among vapour stems, in: Proceedings of the Tenth International Heat Transfer Conference, Vol. 5, Brighton, England, 1994, pp. 135–140.

[24] M.S. El-Genk, A.G. Glebov, Zh. Guo, Pool boiling from downward-facing curved surface in saturated water, in: Proceedings of the Tenth International Heat Transfer Conference, Vol. 5, Brighton, England, 1994, pp. 45–50.

[25] Kang, S., Bartch, G., Jia, D. and Chen, X.-J., Probability model to describe pool boiling phenomena, in: Proceedings of the Tenth International Heat Transfer Conference, Vol. 5, Brighton, England, 1994, pp. 93–98.

[26] C. Corty, A.S. Foust, Surface variables in nucleate boiling, Chemical Engineering Progress Symposium Series (1955) 51 (17) 1–12.

[27] W.M. Rohsenow, J.P. Hartnett, Y.I. Cho (Eds.), Handbook of Heat Transfer, 3rd ed., McGraw-Hill, New York, 1998.

[28] G.F. Hewitt, G.L. Shires, T.R. Bott, Process Heat Transfer, CRC Press, Boca Raton, FL, Begell House, New York, 1994.

[29] ASHRAE Handbook. Fundamentals, American Society of Heating, Refrigeration and Air-Conditioning Engineers, Atlanta, 1997.

[30] M. Kurtz (Ed.), Mechanical Engineering Handbook, John Wiley & Sons, New York, 1998.

[31] J.G. Collier, J.R. Thome, Convective Boiling and Condensation, 3rd ed., Clarendon Press, Oxford, 1994.

[32] L.S. Tong, Y.S. Tang, Boiling Heat Transfer and Two-Phase Flow, 2nd ed., Taylor & Francis, 1997.

[33] F.M. White, Heat and Mass Transfer, Addison Wesley, Reading, MA, 1991.

[34] Mikhailov, M.D., and Özisik, M.N., Heat Transfer Solver, Prentice-Hall, Englewood Cliffs, NJ, 1991.

[35] A. Bejan, Heat Transfer, John Wiley & Sons, New York, 1993.

[36] A.F. Mills, Heat and Mass Transfer, Irwin, Chicago, 1995.

[37] F.P. Incropera, D.P. DeWitt, Fundamentals of Heat and Mass Transfer, 4th ed., John Wiley & Sons, New York, 1996.

[38] J.P. Holman, Heat Transfer, McGraw-Hill, New York, 1997.

[39] J.E. Myers, D.L. Katz, Boiling coefficients outside horizontal tubes, Chemical Engineering Progress Symposium Series (1953) 49 (5) 107–114.

[40] H.H. Ryffel (Ed.), Machinery's Handbook, 22nd ed., Industrial Press, New York, 1984.

[41] L.C. Thomas, Heat Transfer, Prentice-Hall, Englewood Cliffs, NJ, 1992.

[42] Y. Lee, I. Pioro, Ch.-S. Yim, Effect of conjugation on critical heat flux of two-phase closed thermosyphons, in: Proceedings of the 10th International Heat Transfer Conference, Vol. 6, Brighton, England, 1994.